Evolution of high current, cold cathode diodes to steady state

R. E. Shefer, L. Friedland,[a] and R. E. Klinkowstein
Science Research Laboratory, Inc., Somerville, Massachusetts 02143

(Received 22 September 1986; accepted 12 October 1987)

A theoretical model of cathode plasma behavior in a planar, high current, space-charge limited diode is presented. The model predicts the evolution of the cathode plasma to steady state when certain diode conditions are satisfied. This steady state corresponds to current extraction from a stationary plasma boundary with no diode impedance collapse. In order for the equilibrium to be achieved, the driving impedance of the external power supply circuit must be smaller than a critical value that depends only on diode voltage, gap spacing, and plasma electron temperature. The temporal evolution of the cathode plasma is described using both a discrete numerical simulation model and an approximate analytical solution to the transport equations. The dependence on plasma temperature, neutral gas density and composition, diode voltage, gap spacing, and extracted current density are investigated.

I. INTRODUCTION

Cold cathodes have been widely used to provide high current density electron beams for excimer lasers, free electron lasers, flash x-ray sources, and ion diodes. Applications of cold cathode technology have been limited by the impedance collapse of the high voltage diode caused by the expansion of the cathode plasma into the anode–cathode gap. Cathode plasma expansion has been characterized experimentally[1–10] and expansion velocities in the 10^6–10^7 cm/sec range have been measured. Since diode gap spacings are typically of order 0.1–10 cm, electron beam pulse lengths from cold cathodes usually cannot exceed 100 nanoseconds to one microsecond. In addition, the decrease in diode impedance during the pulse means that complicated pulse forming networks must be used in order to ensure efficient transfer of energy from the driving power supply to the diode.

In this paper a theoretical model of cathode plasma behavior in a space-charge limited planar diode is presented. In Sec. II, the model is used to predict a steady state, corresponding to a stationary cathode plasma during current extraction. Conditions for steady state are given in terms of source parameters, degree of ionization, and impedance of the driving power supply. In Sec. III, a numerical simulation scheme is developed to describe the temporal evolution of the plasma to steady state. Finally in Sec. IV a simplified analytic, time-dependent model of the diode is presented and compared with the results of the simulations.

The mechanism of plasma formation at cold cathode surfaces has been discussed extensively in the literature.[2,10–12] Plasma formation is thought to be initiated at microscopic cathode surface imperfections and impurity or grain boundaries, where the enhanced microscopic electric field is high enough for true field emission of electrons from the surface. It is not the intent of this work to describe the initial formation of the cathode plasma in a high voltage diode. In the model presented in the following sections, it is assumed that the initial surface breakdown has occurred and that the resulting plasma layer is spatially uniform. Since plasma is formed throughout the duration of the discharge, a simplified electron impact ionization source is postulated in the model. This source assumes a supply of neutral atoms at the cathode surface and is characterized by a single effective ionization rate coefficient. This rate coefficent represents a multitude of processes including bulk and plasma–surface interactions that are too complicated to treat in detail. By simplifying the plasma source region in this way, it is possible to arrive at a tractable set of equations to describe the evolution of the cathode plasma without loss of generality.

The diode model described in the following sections requires only that the source layer be weakly ionized and occupy a thin region close to the cathode surface. The assumption of weak ionization may be justified *a posteriori* by comparing the steady state plasma density at the cathode to the required neutral gas density. If the neutral density is much higher than the plasma density, neutrals will not come into thermal equilibrium with the electrons and will be characterized by the temperature of the cathode surface, of order $\frac{1}{10}$ eV. The rate of expansion of the gas layer can then be calculated and its thickness is found to be much smaller than the thickness of the plasma layer for the typical diode parameters and time scales of interest.

The presence of neutral gas originating at the cathode in cold cathode diodes is well established. During the discharge, the expansion of the neutral layer is affected by ionization and charge exchange with the ionic species. In addition, local heating and ablation of plasma formation sites at the cathode surface may result in directed flows of ion and neutral atoms. Indeed, fast neutral components have been observed in cathode plasmas.[10] In this model it is assumed that the fast neutral component in the diode is small and that ionization of these neutrals does not significantly affect the diode dynamics.

II. STEADY STATE MODEL

A. Steady state for constant applied voltage

In this model we consider a plasma formed in a parallel plate high voltage diode with a cold cathode, as shown in Fig. 1. The anode–cathode gap ($0<x<L$) is divided into three regions, the vacuum gap ($\bar{x}<x<L$) which contains

[a] Permanent address: Center for Plasma Physics, Racah Institute of Physics, Hebrew University, Jerusalem, Israel.

 0031-9171/88/040930-10$01.90

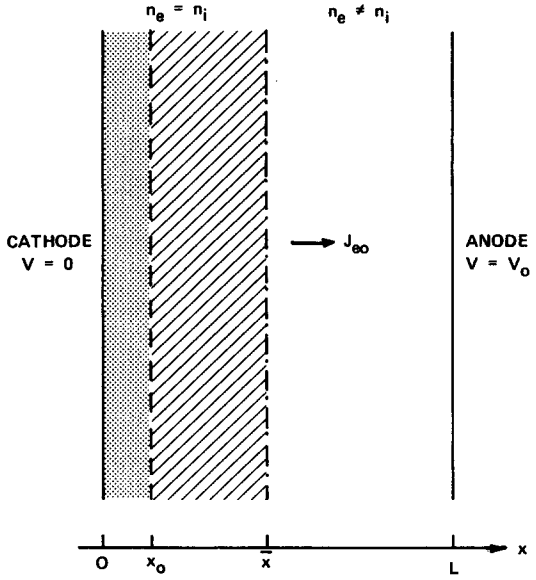

FIG. 1. One-dimensional planar diode with plasma cathode showing gas layer $0 < x \leqslant x_0$, plasma layer $x_0 < x \leqslant \bar{x}$, and vacuum gap containing space-charge limited flow $\bar{x} < x < L$.

the space-charge limited electron flow, a source-free plasma layer ($x_0 < x \leqslant \bar{x}$), and a neutral gas and plasma layer ($0 < x < x_0$) which provides a source of electrons and ions. It is assumed that $x_0 \ll \bar{x}$, that the diode is infinite in the transverse dimensions, and that the charged particle current is continuous everywhere.

The condition for a steady state, stationary plasma boundary corresponds to the situation in which the diode potential is monotonically increasing between the cathode and anode planes. In this case electrons that enter the vacuum gap are accelerated towards the anode plane, while ions are confined by the electrostatic potential of the diode electric field. Electrons enter the gap at a rate determined by their random flux, since under space-charge limited conditions the diode electric field is approximately zero at the emitting surface. Therefore, the random flux must equal the Child–Langmuir flux of electrons accelerated toward the anode plane

$$n_s v_e = \alpha V^{3/2}/(L - \bar{x})^2. \tag{1}$$

The plasma density n_s at the boundary may be calculated from this expression, where $v_e = (T_e/2\pi m)^{1/2}$ is the characteristic velocity of a Maxwellian electron distribution, V is the applied potential, and $\alpha = 2.33 \times 10^{-6}/e$ in mks units. The relativistic correction[13] to the Child–Langmuir expression (1) is not included in this work. This correction does not affect the conclusions that follow.

The continuity equations for both species may be written in the source-free plasma layer ($x_0 < x \leqslant \bar{x}$) as follows:

$$\frac{\partial n}{\partial t} = -\frac{\partial \Gamma_i}{\partial x}, \quad \frac{\partial n}{\partial t} = -\frac{\partial \Gamma_e}{\partial x}, \tag{2a}$$

where, in the diffusion approximation,

$$\Gamma_i = \mu_i n E - D_i \frac{\partial n}{\partial x}, \quad \Gamma_e = -\mu_e n E - D_e \frac{\partial n}{\partial x}. \tag{2b}$$

The subscripts (i,e) refer to ion and electron quantities, respectively, and $n = n_e = n_i$. Since current is continuous,

$$\Gamma_e - \Gamma_i = \Gamma_{e0}, \tag{3}$$

where Γ_{e0} is the extracted electron flux.

In the steady state ($\partial n/\partial t = 0$), $\Gamma_i = 0$ at the plasma boundary $x = \bar{x}$. Therefore, $\Gamma_i = 0$ everywhere in the source-free region. The steady state density profile can then be obtained for $x_0 < x \leqslant \bar{x}$ for two different dependencies of the transport coefficients μ and D on density.

Case (a). Weakly ionized plasma: In this case μ and D are independent of n and Eqs. (2) yield a linear density profile,

$$n(x) = n(x_0) - (\mu_i/\mu_e)(\Gamma_{e0}/D_a)x, \tag{4}$$

where

$$D_a = (\mu_i D_e + \mu_e D_i)/(\mu_i + \mu_e) \simeq D_i(1 + T_e/T_i) \tag{5}$$

is the usual ambipolar diffusion coefficient.

Case (b). Highly ionized plasma: In this case, Coulomb collisions are dominant and μ and D are proportional to $1/n$. Then,

$$n(x) = n(x_0)\exp[-(x - x_0)/\Delta], \tag{6}$$

where

$$\Delta = [(1 + T_i/T_e)D_0]/\Gamma_{e0}$$

and $D_0 = nD_e$.

The remainder of this work will deal primarily with case (b) above since a large neutral atom population is not expected to diffuse to the source-free plasma layer on the time scales of interest. Neutrals may also reach the plasma layer through charge exchange interactions in the gas layer that may be resonant and, therefore, have a high cross section. However, as long as the gas density in the source layer is high these charge exchange neutrals will thermalize quickly, so it is expected that the population of hot neutrals that reaches the plasma layer will be very small. Under these conditions, Coulomb interactions are dominant for the plasma electrons and ions.

The quantity $n(x_0)$ may be determined by solving for the plasma density profile in the weakly ionized gas layer ($0 < x \leqslant x_0$). In this region, the ion continuity equation in (2) is replaced by

$$\frac{\partial n}{\partial t} = -\frac{\partial \Gamma_i}{\partial x} + n n_a \langle \sigma v \rangle_i, \tag{7}$$

where n_a is the neutral gas density and $\langle \sigma v \rangle_i$ is an effective ionization rate coefficient. Here it will be assumed for simplicity that n_a is spatially uniform and is constant in time, that is, there is no significant depletion of the gas reservoir during the discharge. From the expressions for Γ_i and Γ_e in Eq. (2), the ion flux may be written as

$$\Gamma_i = -D_a \frac{\partial n}{\partial x} - \left(\frac{\mu_i}{\mu_i + \mu_e}\right)\Gamma_{e0}$$

$$\simeq -D_a \frac{\partial n}{\partial x} - \frac{\mu_i}{\mu_e}\Gamma_{e0}. \tag{8}$$

Equations (7) and (8) may then be combined to yield the following equation for the density profile in the region $0 < x \leqslant x_0$:

$$\frac{\partial^2}{\partial x^2} n = -k^2 n, \tag{9}$$

where

$$k^2 = n_a \langle \sigma v \rangle_i / D_a.$$

Since collisions with neutral atoms are dominant, D_a is independent of n in this region. Equation (9) is solved using the continuity conditions for the total current and density on the boundaries, i.e., n is continuous at $x = x_0$, $\Gamma_i = 0$ at $x = x_0$, and $\Gamma_i = -\Gamma_{e0}$ at $x = 0$. The last condition states that current is returned to the cathode through ion flux only, which is a good assumption as long as the potential drop in the cathode sheath is much larger than the electron thermal velocity. The plasma density profile in the gas layer may then be obtained:

$$n(x) = \frac{\Gamma_{e0}}{k} \frac{\mu_e}{(\mu_i D_e + \mu_e D_i)} \times \left(\mu_i \sin kx + \frac{\mu_i + \mu_e \cos kx_0}{\sin kx_0} \cos kx \right). \tag{10}$$

In order for Γ_i to equal $-\Gamma_{e0}$ at $x = 0$, the plasma must be capable of supplying the required random ion flux. If the ions are Maxwellian, then

$$n(0) = \Gamma_{e0} / v_i, \tag{11}$$

where $v_i = (T_i / 2\pi m)^{1/2}$. This additional condition makes it possible to relate the electron and ion temperatures to the neutral gas density through the following expression:

$$\frac{1}{(\mu_i D_e + \mu_e D_i)} \frac{\mu_i + \mu_e \cos kx_0}{k \sin kx_0} = \frac{1}{v_i}. \tag{12}$$

For $\mu_i / \mu_e \ll 1$, Eq. (12) can be simplified to yield an explicit relationship between n_a, T_e, and T_i:

$$n_a x_0 = (v_i / \langle \sigma v \rangle_i \xi) \tan^{-1} \xi, \tag{13}$$

where

$$\xi = (v_i / v_e)^{1/2} (\lambda_{\text{ion}} / \lambda_{\text{el}})^{1/2}$$

and λ_{ion} and λ_{el} are the mean free paths for electron impact ionization and ion-neutral elastic collisions, respectively. The quantity ξ is a function of T_e and T_i only and is a measure of the degree of collisionality of the ions. In the limit of collisionless ions, $(1/\xi) \tan^{-1} \xi \to 1$, and Eq. (13) is immediately recognizable as a statement of particle balance in the gas layer. In Fig. 2, the line density of hydrogen gas atoms $n_a x_0$ calculated from Eq. (13) is plotted as a function of the electron temperature for $T_i = T_e$. The measured[10] temperature range for cathode plasmas, 3–6 eV, corresponds to a hydrogen gas surface coverage of 0.5 to 10 monolayers.

In the approximation $\mu_i / \mu_e \ll 1$, the plasma density profiles in the gas and plasma region, Eq. (10) and Eq. (7) may be written as

$$n(x) = n(0) \xi [\sin kx + (1/\xi) \cos kx] \quad (0 < x \leqslant x_0), \tag{14}$$

$$n(x) = n(0)(1 + \xi^2)^{1/2} \exp[-(x - x_0)/\Delta] \quad (x_0 < x \leqslant \bar{x}), \tag{15}$$

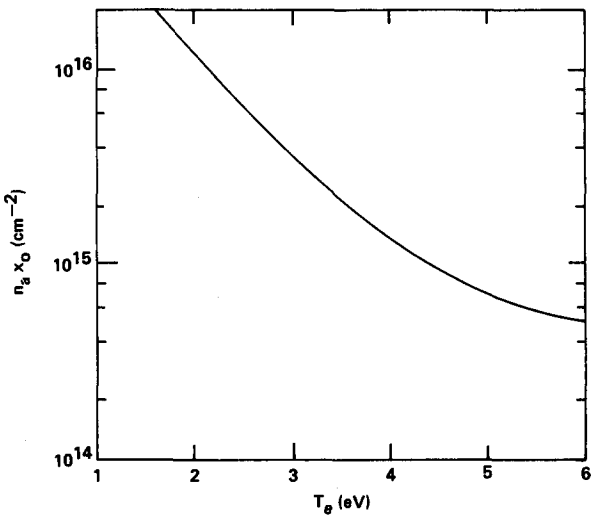

FIG. 2. Steady state neutral gas inventory $n_a x_0$ from Eq. (13) as a function of electron temperature T_e for a hydrogen plasma with $T_i = T_e$.

density at $x = x_0$ has been used to obtain the coefficient of the exponential in Eq. (15).

The condition for a stationary plasma boundary at $x = \bar{x}$ is that the extracted space-charge limited electron flux Γ_{e0} equal the random flux of electrons into the vacuum gap, $\Gamma_{e0} = n(\bar{x}) v_e$. Using this boundary condition, the steady state size of the plasma layer may be written in terms of the extracted flux

$$\bar{x} - x_0 = (1 + T_i/T_e)(D_0/\Gamma_{e0}) \ln A = \Delta \ln A, \tag{16}$$

where

$$A \equiv (1 + \xi^2)^{1/2} v_e / v_i.$$

Equation (16) indicates that the steady state location of the plasma boundary is inversely proportional to the extracted flux and is a strong function of the electron temperature through the electron diffusion coefficient $D_0 \propto T_e^{5/2}$. The atomic physics processes in the source region, or gas layer, only enter into Eq. (16) in the argument of the logarithm, so that the functional dependence of $\bar{x} - x_0$ on the details of these processes is very weak.

Combining Eq. (16) with Eq. (6), the ratio of the plasma density at the cathode to the density at the extraction boundary may be written in terms of the electron and ion temperatures as

$$n(\bar{x})/n(x_0) = e^{-(\bar{x} - x_0)/\Delta} = 1/A.$$

The minimum value of A is the square root of the ion to electron mass ratio and A increases with decreasing plasma temperature. Thus the steady state model predicts a steep plasma density gradient—typically several orders of magnitude.

The assumption of weak ionization ($n_a \gg n$) and thin spatial extent of the gas layer ($x_0 \ll \bar{x}$) may now be examined by looking at Eqs. (13), (15), and (16). For example, for a diode with $V = 1$ MV, $L = 2$ cm, $J_{e0} = 1$ kA/cm^2, and $T_e = 2$ eV, it is found that $n_a x_0 = 1.2 \times 10^{16}$ cm^{-2} from Eq. (13), $\bar{x} - x_0 = 0.6$ cm from Eq. (16) and $n(x_0) \simeq 10^{16}$ cm^{-3}. For a neutral gas temperature of 0.1 eV, the gas kinetic diffusion rate for hydrogen will be approximately 10^{-2}

cm/μsec. Therefore, after 10 μsec, $x_0 = 0.1$ cm and $n_a \simeq 10^{17}$ cm^{-3}, and the model assumptions are still satisfied.

The explicit dependence of the quantity $\bar{x} - x_0$ on the physical diode parameters, gap spacing L, and applied voltage V, may be obtained by substituting for the electron flux $\Gamma_{e0} = \alpha V^{3/2}/(L - \bar{x})^2$ in Eq. (16):

$$\bar{x} - x_0 = L + \frac{1}{2Q \ln A} - \left(\frac{L}{Q \ln A} + \frac{1}{4Q^2 \ln^2 A} \right)^{1/2}, \tag{17}$$

where

$$Q \equiv D_0(1 + T_i/T_e)/\alpha V^{3/2}.$$

An interesting property of Eq. (17) is that the solutions have $\bar{x} - x_0 < L$ for all values of the quantities Q and A. Therefore, for a highly ionized plasma in a space-charge limited diode, there is always a steady state for some value of extracted current density $e\Gamma_{e0}$. This may be contrasted with the case of the weakly ionized plasma for which the steady state density profile is linear [Eq. (4)]. In this case, the expression for $\bar{x}$, the location of the plasma boundary, is

$$\bar{x} - x_0 = [(\mu_i + \mu_e)/\mu_i](D_a/v_e)(A - 1), \tag{18}$$

which is independent of the extracted flux Γ_{e0}. In this case, plasma conditions may exist for which $\bar{x} > L$ and there is no steady state.

B. Steady state for finite driving impedance

In the foregoing discussion it is assumed that the applied anode–cathode voltage V does not depend on the extracted current. In this section a more general case will be examined in which the driving power supply has an output impedance Z_0 and the diode voltage V is related to the applied voltage V_0 through

$$V(t) = V_0 - eZ_0 S \Gamma_{e0}(t), \tag{19}$$

where S is the cathode area. Using the equation for the steady state plasma size [Eq. (16)] along with the Child–Langmuir relation and Eq. (19), the following implicit expression for the electron flux Γ_{e0} is obtained:

$$L\Gamma_{e0} - D_0(1 + T_i/T_e)\ln A = \alpha^{1/2}\Gamma_{e0}^{1/2}(V_0 - Z_0 eS\Gamma_{e0})^{3/4}. \tag{20}$$

Equation (20) has a real solution for Γ_{e0} only when the following condition is satisfied,

$$Z_0 < Z_{cr},$$

where

$$Z_{cr} = LV_0/[D_0(1 + T_i/T_e)(\ln A)eS]. \tag{21}$$

Equation (21) indicates that in order for a steady state solution to exist in a high voltage diode with anode–cathode spacing L and applied voltage V_0, the driving impedance must be smaller than a critical value that depends only on L, V_0, and the electron and ion temperatures in the discharge. This may be understood physically in the following way. After a discharge is initiated, the gap voltage V_0 will decrease by an amount proportional to the driving impedance Z_0. This will cause Γ_{e0} to drop and $\bar{x}$ to increase accordingly. That is, the right-hand side of Eq. (1) may never be large enough to balance the random flux of electrons, which is a function only of the discharge parameters. Figure 3 shows the critical impedance as a function of electron temperature for $T_i = T_e$ for a diode with a 2.5 cm gap and a 100 cm^2 emitting area at an applied voltage of 300 kV. It is evident from Fig. 3 that in order to maintain a high Z_{cr}, T_e must be low, which means that the source region of the discharge must be rich in neutral gas, as shown in Fig. 2.

III. TEMPORAL EVOLUTION OF THE PLASMA

In this section, the temporal evolution of the plasma is considered. Since the evolution takes place on the slow ambipolar diffusion time scale and because of the high electron mobility, it will be assumed that the total current is quasistationary at all times,

$$\Gamma_e(x,t) - \Gamma_i(x,t) = \Gamma_{e0}(t),$$

where $\Gamma_{e0}(t)$ is the instantaneous value of the electron extraction flux from the plasma boundary at time t. Then, again, the last two equations in (2) yield expression (8) for the ion particle flux Γ_i, with $\Gamma_{e0} = \Gamma_{e0}(t)$. In contrast to the steady state, of course, $\Gamma_i \neq 0$ in the time-dependent case considered in this section.

The numerical modeling of the expanding plasma in the diode is accomplished through the development of a discrete plasma model that may easily be adapted to numerical computations. Again, a planar anode–cathode gap is considered with gap spacing L and infinite transverse dimensions. This gap is divided into a number of equally spaced planes a distance δ apart, as shown in Fig. 4. The plasma density in the gap $n(x_k)$ is then expressed as a surface density of particles on the k th plane located at $x = x_k$,

$$N_k = n(x_k)\delta. \tag{22}$$

Plasma particles are allowed to move to the left or right of the k th plane with probabilities per unit time equal to a_k and

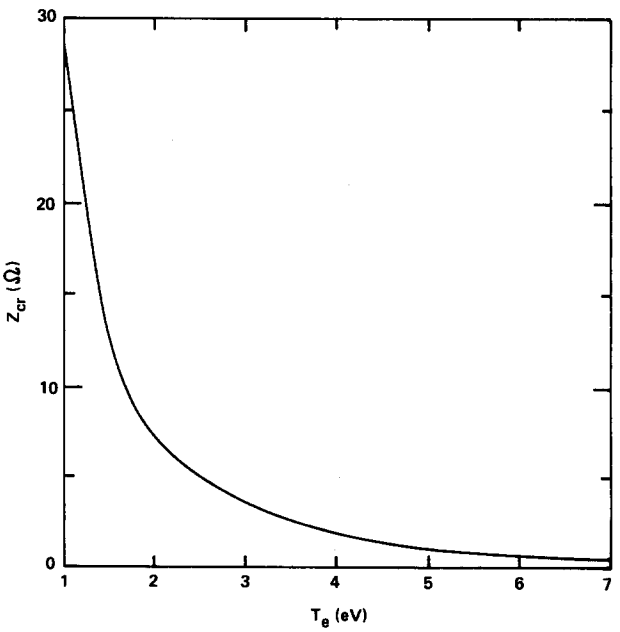

FIG. 3. Critical driving impedance Z_{cr} from Eq. (21) as a function of electron temperature T_e for $T_i = T_e$. Diode parameters are $L = 2.5$ cm, $V_0 = 300$ kV, and $S = 100$ cm^2.

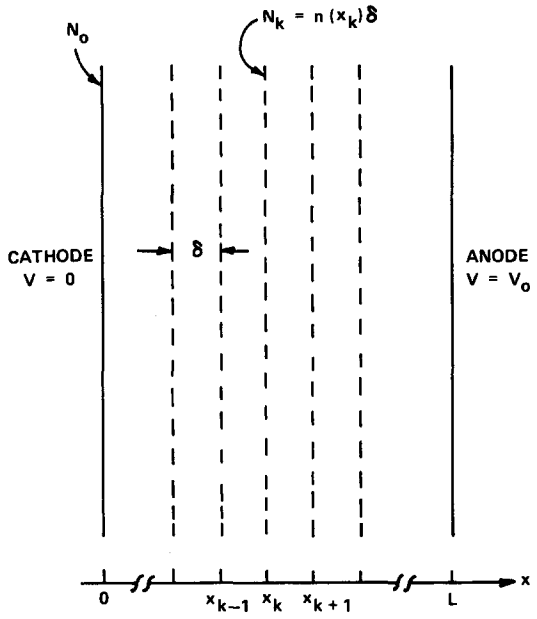

FIG. 4. Schematic of discrete plasma model geometry used in numerical simulations of temporal plasma evolution.

b_k, respectively. The surface density on the kth plane then satisfies the model transport equation,

$$\frac{\partial N_k}{\partial t} = -a_k N_k - b_k N_k + a_{k+1} N_{k+1} + b_{k-1} N_{k-1}. \tag{23}$$

It remains to relate the a and b probabilities to the usual transport coefficients μ and D in the plasma. This is accomplished by Taylor expanding Eq. (23) in the small parameter δ for the two cases discussed in Sec. II.

Case (a). Weakly ionized plasma: In this case Eq. (23) may be expanded directly:

$$\frac{\partial N_k}{\partial t} = -\frac{\partial}{\partial x}\left[\left(\delta(b_k - a_k) - \frac{1}{2}\delta^2 \frac{\partial}{\partial x}(a_k + b_k)\right)N_k - \frac{1}{2}\delta^2 (a_k + b_k)\frac{\partial N_k}{\partial x}\right] + O(\delta^3). \tag{24}$$

Comparing Eq. (24) with the first equation in (2), where Γ_i is given by Eq. (4), yields the following interpretation of a_k and b_k:

$$a_k = \frac{D_a}{\delta^2} + \frac{\Gamma_{e0}}{2N_k}\left(\frac{\mu_i}{\mu_i + \mu_e}\right),$$
$$b_k = \frac{D_a}{\delta^2} - \frac{\Gamma_{e0}}{2N_k}\left(\frac{\mu_i}{\mu_i + \mu_e}\right). \tag{25}$$

Here it has been assumed that D_a is a constant. The position x for which b_k equals zero corresponds to the transition to the space-charge limited sheath and b_k is set to zero for all $x_k > \bar{x}$ since the plasma in this region is no longer described by the diffusion equation.

Case (b). Highly ionized plasma: For a plasma dominated by Coulomb collisions, the transport coefficients are proportional to $1/n$. The problem is considerably simplified by defining the quantities α_k and β_k as

$$\alpha_k \equiv a_k N_k \quad \text{and} \quad \beta_k \equiv b_k N_k. \tag{26}$$

Then the model transport equations become

$$\frac{\partial N_k}{\partial t} = -\alpha_k - \beta_k + \alpha_{k+1} + \beta_{k-1}. \tag{27}$$

Following the same procedure as in case (a), i.e., expanding $\alpha_{k+1}, \beta_{k-1}$ in powers of δ, α_k, and β_k may again be related to the plasma transport coefficients:

$$\alpha_k = \frac{1}{2}\Gamma_{e0}\left(\frac{\mu_i}{\mu_i + \mu_e}\right) + \frac{D_{a0}}{\delta}\ln\frac{N_i}{N^*},$$
$$\beta_k = -\frac{1}{2}\Gamma_{e0}\left(\frac{\mu_i}{\mu_i + \mu_e}\right) + \frac{D_{a0}}{\delta}\ln\frac{N_i}{N^*}. \tag{28}$$

Here $D_{a0} = nD_a$ and N^* is a normalizing constant determined by setting $n = \Gamma_{e0}/v_e$ for $x = \bar{x}$ giving $N^* = (\Gamma_{e0}/v_e)\exp(-\Gamma_{e0}\delta/2D_{a0})$.

A simple computational procedure may now be used to determine the temporal evolution of the plasma layer. At time $t = 0$, all plasma particles reside on the source plane at $x_k = 0$. On each subsequent time step, the densities N_k are calculated from Eq. (23) or Eq. (27) using the coefficients calculated from Eq. (25) or Eq. (28).

The plasma density at the source plane, $N_0 = n_0\delta$, is determined from the ion continuity equation in the source region,

$$\frac{\partial n_0}{\partial t} = -\frac{\partial \Gamma_0}{\partial x} + n_0 n_a \langle \sigma v \rangle_i. \tag{29}$$

The processes by which the electron density in the source layer adjusts to provide the required electron flux are governed by the electron temperature, which in turn is controlled by the discharge electric field. Therefore, particle balance in the source layer will be established on a time scale that is rapid compared with the time scale of the expansion of the plasma boundary, since this expansion is governed by the motion of the more massive ions. Hence, it is assumed in modeling the expansion of the plasma layer that the source layer is in quasiequilibrium and $\partial n_0/\partial t = 0$. The source density at a given time is then given by the electron balance equation,

$$N_0 = G\Gamma_{e0}\delta/n_a x_0 \langle \sigma v \rangle_i, \tag{30}$$

where

$$G = \frac{n_0 x_0}{\int_0^{x_0} n(x)\,dx}.$$

As before, the neutral gas density n_a and the electron and ion temperatures are related through Eq. (13) and the factor G describes the nonuniformity of the plasma density in the source region [see Eq. (10)]. (Note that $G \to \pi/2$ when $\xi \to \infty$ and $G \to 1$ when $\xi \to 0$.) This "quasiequilibrium" treatment of the source layer completes the discrete time-dependent model of plasma motion in the gap.

The temporal evolution of the cathode plasma layer may now be simulated numerically. Figure 5 shows the evolution of a highly ionized [case (b)] plasma layer in a 1 MV diode with $L = 2$ cm and $T_e = T_i = 2$ eV. In Fig. 5(a), the normalized density profile is seen to evolve to the exponential profile predicted in the steady state model with $\bar{x} = 0.64$ cm

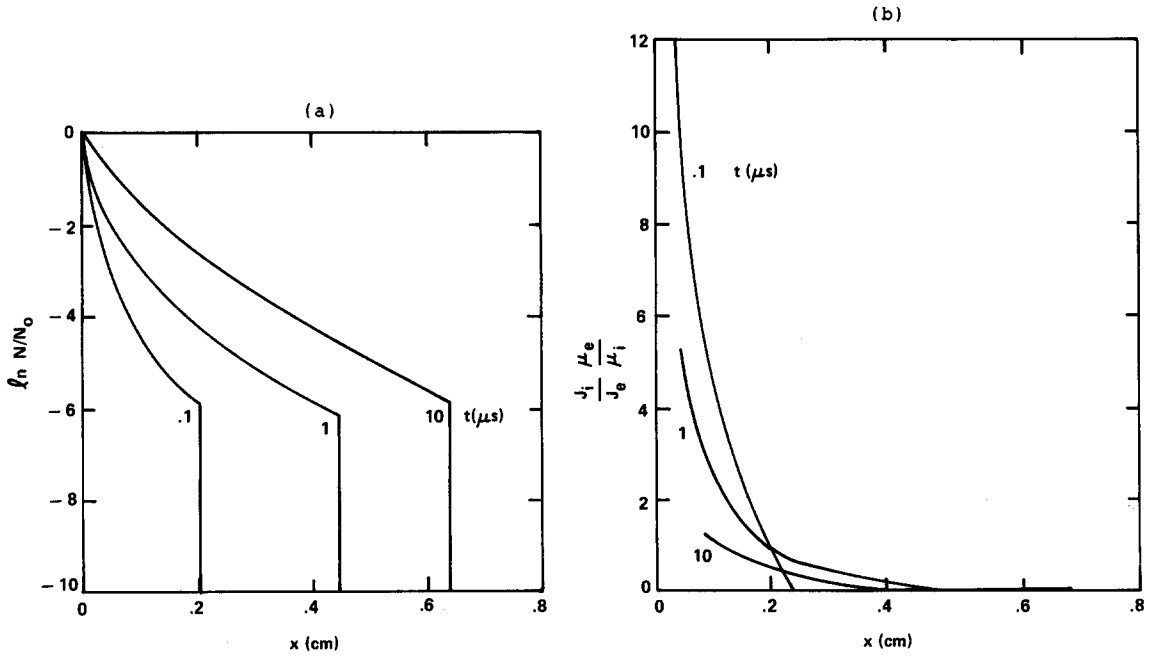

FIG. 5. Temporal evolution of a highly ionized plasma layer for $V = 1$ MV, $L = 2$ cm, $T_i = T_e = 2$ eV: (a) logarithm of plasma density N normalized to density at source plane N_0 as a function of distance from cathode x for $t = 0.1$, 1, and 10 μsec; (b) normalized ion current $J_i\mu_e/J_e\mu_i$ as a function of x for $t = 0.1$, 1, and 10 μsec.

in agreement with Eq. (17). Figure 5(b) shows the ion current, normalized to the electron current and the ratio of the mobilities, as a function of x. The ion current is seen to decrease everywhere in the plasma as a function of time (J_i is always zero at the plasma boundary) so that $J_i \to 0$ for all x as the system evolves to steady state.

Figure 6 shows the time dependence of the diode gap spacing $L - \bar{x}$ and the extracted current density J_{e0}. Both quantities are seen to evolve very rapidly in the initial stages of the discharge ($t = 0$–200 nsec) and thereafter evolve to steady state on a time scale of tens of microseconds. This qualitative behavior is observed in the simulation for a wide range of diode parameters. Indeed, the predicted initial plasma expansion velocity falls in the range 2–4 cm/μsec, in agreement with a large number of experimental observations. Most experimenters, however, have not been able to maintain the diode voltage for times beyond this initial expansion phase. The scaling of the characteristic initial and

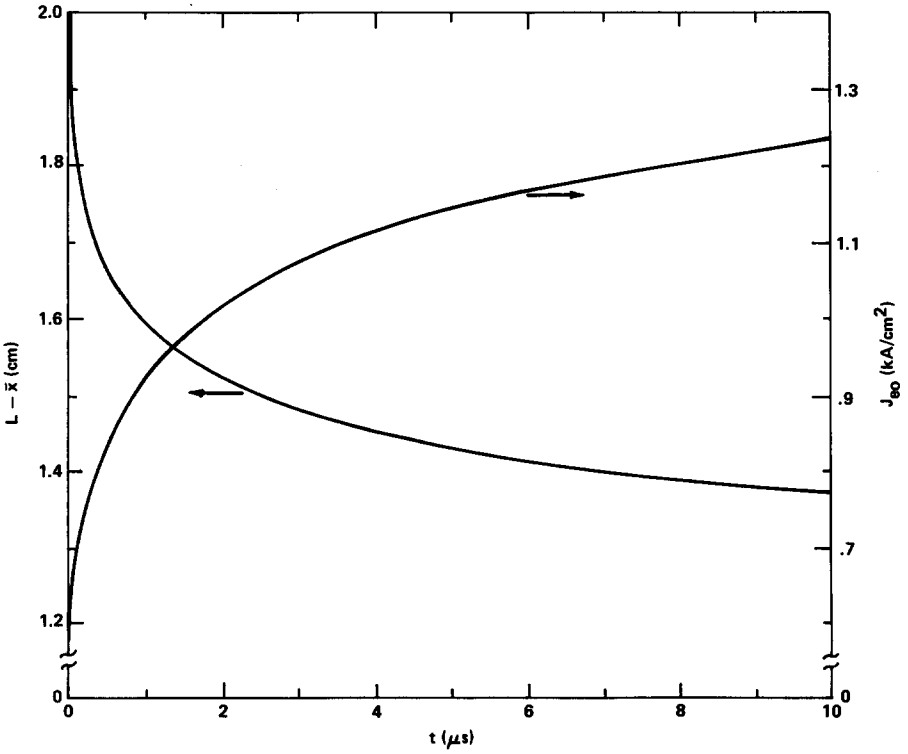

FIG. 6. Vacuum gap $L - \bar{x}$ and extracted current J_{e0} as a function of time for a diode with $V = 1$ MV, $L = 2$ cm, and $T_i = T_e = 2$ eV.

final expansion time scales with various diode parameters is predicted by a semianalytic model of the expanding plasma discussed in Sec. IV of this paper.

In Fig. 7, the evolution of a weakly ionized plasma layer is depicted. The diode parameters are the same as those of the previous example except that the electron motion in the plasma layer is assumed to be governed by collisions with neutral atoms and the electron mean free path is chosen so that a steady state is predicted by Eq. (18) with $\bar{x} = 0.9$ cm. The density profile is seen to evolve to the predicted linear profile at large t with the ion current $J_i \to 0$ everywhere in the plasma.

The numerical simulation technique can also be used to examine the evolution of the cathode plasma in a diode driven by a finite impedance voltage source [Eq. (19)]. Figure 8 shows the temporal evolution of the gap spacing $L - \bar{x}$ for driving impedances Z_0 below and above the critical value given by Eq. (21). In this example the initial gap voltage is 300 kV with a spacing $L = 2.5$ cm and $T_e = T_i = 2$ eV. For

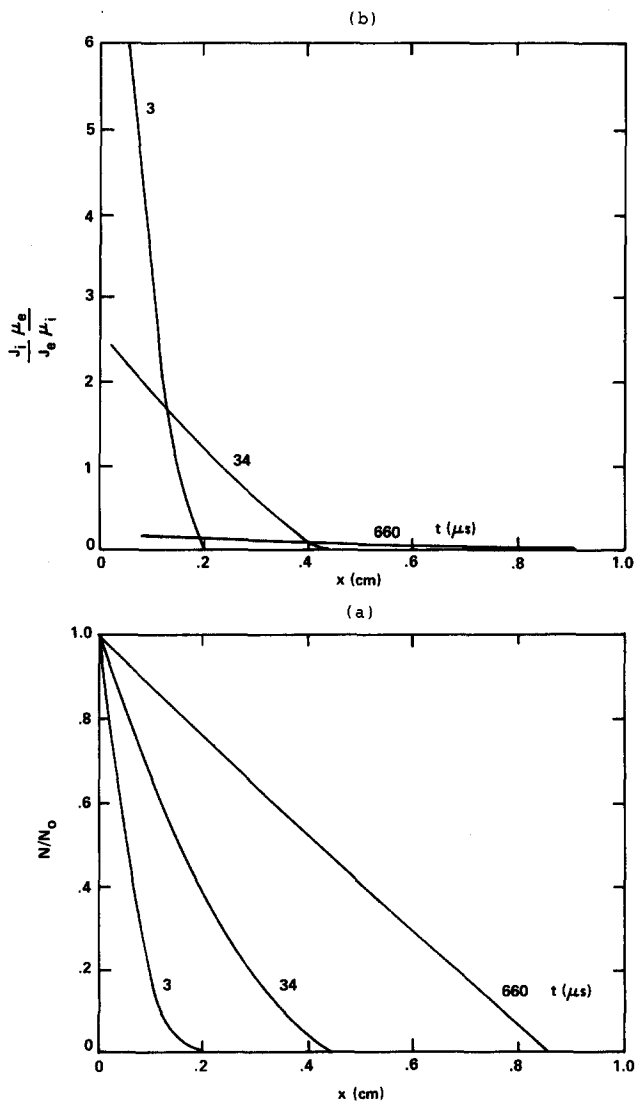

FIG. 7. Temporal evolution of a weakly ionized plasma layer for $V = 1$ MV, $L = 2$ cm, $T_i = T_e = 2$ eV: (a) plasma density N normalized to density N_0 at source plane as a function of distance from cathode x for $t = 3$, 34, and 660 μsec; (b) normalized ion current $J_i\mu_e/J_e\mu_i$ as a function of x for $t = 3$, 34, and 660 μsec.

$Z_0 = 0$ this system reaches steady state with $L - \bar{x} \simeq 1$ cm. For $Z_0 = 50\ \Omega$, $Z_0 > Z_{cr}$, and $L - \bar{x} \to 0$ corresponding to diode impedance collapse. Thus Fig. 8 illustrates the importance of low driving impedance in the operation of a long pulse cold cathode diode.

IV. ANALYTIC MODEL OF THE EXPANDING PLASMA LAYER

In this section an analytic solution to the diffusion equation is developed for the highly ionized plasma case. The diffusion equation in the source-free region is

$$\frac{\partial n}{\partial t} = D\frac{\partial^2}{\partial x^2}(\ln n), \tag{31}$$

where

$$D = (\mu_i/\mu_e)(1 + T_i/T_e)D_0.$$

The solution may be sought by writing $n(x,t)$ in the form

$$n(x,t) = n_0(t)e^{\psi(x,t)}, \tag{32}$$

where $n_0(t)$ describes the time-dependent density at $x = x_0 \simeq 0$. It is assumed in Eq. (32) that at all times

$$\psi(x_0,t) \simeq \psi(0,t) \equiv 0. \tag{33}$$

In addition, the quasistationary condition (30) can again be exploited. This condition can be written as

$$n_0(t)/n(\bar{x}(t),t) = v_e G/n_a x_0 \langle \sigma v \rangle_i \equiv A, \tag{34}$$

where A is given in Eq. (16), and $\bar{x}(t)$ is the time-dependent position of the electron current extraction boundary of the plasma layer. Thus

$$\psi(\bar{x}(t),t) = -\ln A. \tag{35}$$

Equations (33) and (35) constitute the spatial boundary conditions on the function $\psi(x,t)$.

The x dependence of ψ may be approximated by the quadratic

$$\psi \simeq -P(t)x + R(t)x^2. \tag{36}$$

For $x/\bar{x} \ll 1$, Eq. (36) can be viewed as a truncated expan-

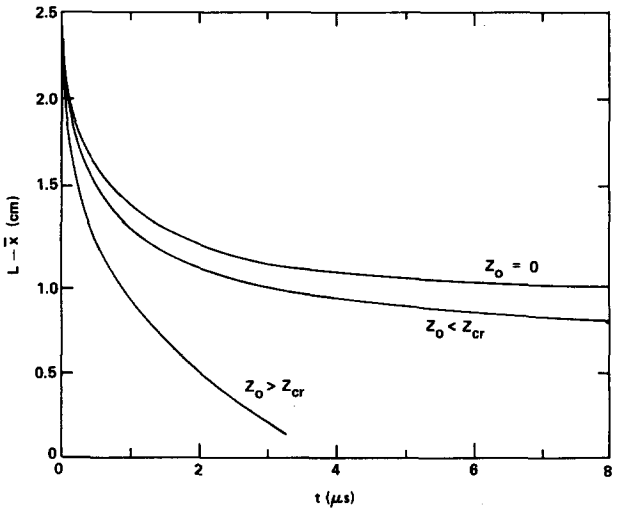

FIG. 8. Vacuum gap $L - \bar{x}$ as a function of time for $V = 300$ kV, $L = 2.5$ cm, and $T_i = T_e = 2$ eV. Curves shown are for $Z_0 = 0$, $Z_0 = 4\ \Omega$ ($Z_0 < Z_{cr}$), and $Z_0 = 50\ \Omega$ ($Z_0 > Z_{cr}$).

sion of ψ in powers of x at a given time t. The coefficients $R(t)$ and $P(t)$ may be found by using the diffusion equation along with the expression for the ion flux. Indeed, Eq. (31) now becomes

$$\frac{dn_0}{dt}+\frac{\partial\psi}{\partial t}n_0e^{\psi}=D\frac{\partial^2\psi}{\partial x^2}, \tag{37}$$

which, on using Eq. (36) and expanding in powers of x, yields

$$\frac{dn_0}{dt}+O(x)=2DR+O(x) \tag{38}$$

so that

$$R(t)=\frac{1}{2D}\frac{dn_0}{dt}. \tag{39}$$

The expression (4) for the ion current, in the new notation, becomes

$$\Gamma_i=D(P-2Rx)-\Gamma_{e0}\mu_i/\mu_e. \tag{40}$$

Although $\Gamma_i\neq 0$ everywhere, the ion current certainly vanishes at the extraction plasma boundary, $x=\bar{x}(t)$, where the ions are reflected. Thus

$$\Gamma_i(\bar{x},t)=D(P-2R\bar{x})-\Gamma_{e0}\mu_i/\mu_e=0 \tag{41}$$

yielding an expression for $P(t)$:

$$P(t)=(\Gamma_{e0}/D)(\mu_i/\mu_e)+2R\bar{x}. \tag{42}$$

Thus the function ψ has fixed values on the plasma boundaries [$x\simeq 0$, $x=\bar{x}(t)$] and a well defined coefficient in the quadratic term [see Eq. (36)], assuming that the dependence $n_0=n_0(t)$ is known. These constraints on ψ comprise the basis for the use of the quadratic approximation (36) at all times. Equation (36) is consistent with the steady state solution where [see Eq. (6)]

$$P=\frac{1}{\Delta},\quad R=\frac{1}{2D}\frac{dn_0}{dt}=0. \tag{43}$$

A full description of the expanding plasma may now be obtained. Substituting (42) and (39) into (35) gives an expression for dn_0/dt:

$$\frac{dn_0}{dt}=\frac{2D}{\bar{x}^2}\ln A-\frac{\bar{x}(t)}{\Delta(t)}. \tag{44}$$

Here $\Delta(t)$, as in the steady state, is defined in Eq. (6) with the only difference that the time-dependent flux $\Gamma_{e0}(t)$ is used. Finally, $\Gamma_{e0}(t)$ is given by

$$\Gamma_{e0}(t)=\alpha V(t)^{3/2}/(L-\bar{x})^2=v_en_0(t)/A \tag{45}$$

or

$$\bar{x}(t)=L-[\alpha V(t)^{3/2}/v_eAn_0(t)]^{1/2}. \tag{46}$$

Equations (44) and (46) yield the desired time dependence of $n_0(t)$, and, therefore, $\bar{x}(t)$ and $\Gamma_{e0}(t)$. The solution $n_0(t)$ must be found subject to the initial conditions $\bar{x}=0$ and $n_0=\alpha V^{3/2}/L^2v_eA$ at $t=0$. Note that when $\bar{x}$ approaches its equilibrium value ($\bar{x}\to\Delta\ln A$), Eq. (44) correctly predicts $dn_0/dt\to 0$. If, in contrast, the steady state condition cannot be reached, namely, $\ln A$ is always greater than $\bar{x}(t)/\Delta(t)$, then Eq. (44) predicts closure of the diode. Such a case is characteristic of a diode with finite driving impedance in the parameter regime $Z_0>Z_{cr}$ described in Sec. II in which the diode collapse is a result of the rapid decrease of the voltage V with the current.

In general, when the diode voltage V is a function of time (as, for example, in the finite driving impedance case) the solution of Eqs. (44) and (46) must be found numerically. In contrast to the general situation in which $V=V(t)$, a closed form solution of Eq. (44) may be obtained for a constant voltage diode. In this case, Eq. (45) together with Eq. (44) yields

$$\frac{A}{v_e}\frac{d\Gamma_{e0}}{dt}=\frac{2D}{\bar{x}^2}\ln A-\frac{\bar{x}\Gamma_{e0}}{D\mu_i/\mu_e}. \tag{47}$$

By writing

$$\Gamma_{e0}=\beta^2/(L-\bar{x})^2,\quad\text{where}\quad\beta^2\equiv\alpha V^{3/2}, \tag{48}$$

then

$$x=L-\beta/\sqrt{\Gamma_{e0}} \tag{49}$$

and Eq. (47) can be transformed into

$$\frac{d\sqrt{\Gamma_{e0}}}{dt}=\frac{Dv_e}{A}\frac{\sqrt{\Gamma_{e0}}}{(L\sqrt{\Gamma_{e0}}-\beta)^2}\times\left(\ln A-\frac{L\Gamma_{e0}-\beta\sqrt{\Gamma_{e0}}}{D\mu_i/\mu_e}\right). \tag{50}$$

Defining $y\equiv\sqrt{\Gamma_{e0}}$ allows (50) to be written as

$$\frac{dy}{dt}=q\frac{y}{(y-r)^2}[p-y(y-r)], \tag{51}$$

where

$$q\equiv\frac{v_e}{AL\mu_e/\mu_i},\quad p\equiv\frac{D}{L}\frac{\mu_e}{\mu_i}\ln A,\quad r\equiv\frac{\beta}{L}. \tag{52}$$

Equation (51) can be integrated to yield

$$\frac{y_0^2}{y_1y_2}\ln\frac{y}{y_0}+\frac{(y_1-y_0)^2}{y_1(y_1-y_2)}\ln\frac{y-y_1}{y_0-y_1}+\frac{(y_2-y_0)^2}{y_2(y_2-y_1)}\ln\frac{y-y_2}{y_0-y_2}=-qt, \tag{53}$$

where $y_0=r=\sqrt{\Gamma_{e0}}\,\big|_{t=0}$ and the $y_{1,2}$ are the roots of the quadratic equation

$$p-y(y-r)=0, \tag{54}$$

that is,

$$y_{1,2}=y_0/2\pm\sqrt{(y_0/2)^2+p}. \tag{55}$$

At this point, it is interesting to examine the behavior of the function $y(t)$ in the limits $t\to 0$ and $t\to\infty$. At short times the solution $y(t)$ can be found directly from Eq. (51) with $y\simeq r=y_0$:

$$y\simeq y_0+(3qrpt)^{1/3}=y_0[1+0.4(47qpt/r^2)^{1/3}]. \tag{56}$$

On the other hand, for large values of t, when $y\to y_1$, Eq. (53) yields

$$y\simeq y_1+y_2\exp\{-[qy_1(2y_1-y_0)/(y_1-y_0)^2]t\}. \tag{57}$$

The initial current growth, then, is described by the time scale

$$\tau_0=r^2/47qp=\alpha^2A/47v_eD\ln A. \tag{58}$$

Here τ_0 is the time in which the current Γ_{e0} increases by a

factor of 2, and is independent of the gap spacing L. At large values of t, in contrast, the current relaxation is described by a typical time scale that is linearly proportional to L:

$$\tau_1 \simeq \frac{(y_1 - y_0)^2}{q y_1 (2y_1 - y_0)} \simeq \frac{1}{2q} = \frac{\mu_e A L}{2\mu_i v_e}, \quad \text{for} \quad y_1 \gg y_0. \tag{59}$$

It is interesting to observe that

$$\frac{\tau_0}{\tau_1} = \frac{2}{3}\frac{r^2}{p} \simeq \frac{2}{47}\frac{y_0^2}{y_1^2} \ll 1$$

so that the initial time scale is much faster than the time scale of the final relaxation to steady state. This behavior is also observed in the numerical simulations.

At this point the results of the numerical simulations of the plasma layer may be compared with the predictions of the semianalytic theory. In Fig. 9, the time dependence of the electron current density in the diode is plotted from the numerical and analytic calculations. Two cases are considered; in case (a), $V = 1$ MV, $L = 1$ cm, and $T_e = T_i = 2$ eV. Case (b) is identical to case (a) except $L = 2$ cm. The figure shows that the semianalytic theory is generally in good agreement (within approximately 10%) with the results of the numerical simulations. Moreover, both models predict the same qualitative behavior of the current, with the rapid initial growth and the relatively slow final relaxation time scale. However, the present semianalytic model does not accurately predict the very rapid initial current growth in the diode when the plasma density gradient is large. This effect is more pronounced in case (a) where the difference between the initial and final diode currents is larger.

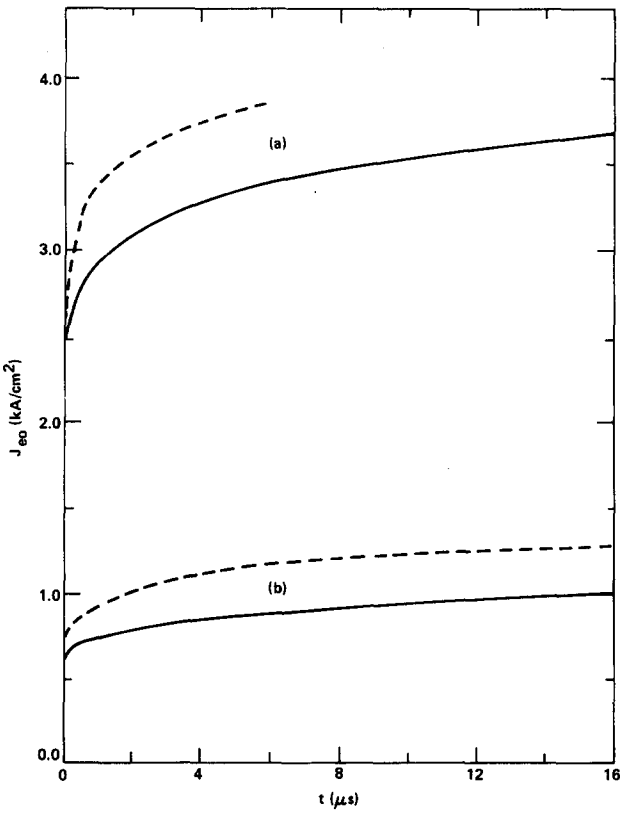

FIG. 9. Extracted current density J_{e0} as a function of time predicted by semianalytic model (solid curves) and numerical plasma simulation (dashed curves). Case (a) has $V = 1$ MV, $L = 1$ cm, $T_i = T_e = 2$ eV, and a predicted steady state current density $J_\infty = 4.18$ kA/cm^2. Case (b) has $V = 1$ MV, $L = 2$ cm, $T_i = T_e = 2$ eV, and $J_\infty = 1.45$ kA/cm^2.

V. DISCUSSION AND CONCLUSIONS

The temporal evolution of a cathode plasma in a planar space-charge limited diode has been described through the use of the fluid equations with a source driven by a single effective ionization rate coefficient. In this model, plasma is produced in a thin, cold, neutral gas layer close to the cathode surface and expands into the anode–cathode gap. The equations describing particle transport in the plasma may be solved analytically for $\partial/\partial t \to 0$ to yield a steady state plasma density profile during current extraction. If the source-free plasma layer is highly ionized, and if the driving voltage is constant a steady state solution may always be found corresponding to current extraction from a stationary plasma boundary with no diode impedance collapse. For typical high current diode parameters, $V \simeq 0.1$–1 MV and plasma temperatures in the range 2–6 eV, this steady state corresponds to a steep plasma density gradient of several orders of magnitude.

The temporal evolution of the plasma layer to steady state has been analyzed in two ways. First, a numerical simulation scheme has been developed in which transport in the plasma is described in terms of the motion of particles between closely spaced planes parallel to the cathode and anode electrodes. Second, a semianalytic time-dependent solution to the diffusion equation is obtained that yields a solution for the time-dependent electron current. Both techniques reveal the same qualitative behavior of the plasma layer; an initial rapid expansion phase corresponding to the typical measured expansion velocities of order 1 cm/μsec followed by a subsequent slow expansion to steady state. The dependence of the two time scales on the physical system parameters may be found from the semianalytic solution. Equation (58) shows that the rapid time scale is a function only of T_e and T_i, with the strongest dependence on T_e through $D \propto T_e^{5/2}$, so that the initial expansion is driven by ambipolar diffusion. The long final relaxation time scale, given by Eq. (59), is a weak function of plasma temperature but depends linearly on L, the initial anode–cathode gap spacing. Thus, for a given diode voltage, higher current discharges evolve more rapidly to steady state.

When the diode voltage is supplied by a power supply with nonzero impedance, the applied voltage is a function of the extracted current and the model predicts a parameter regime in which no steady state solution to the diffusion equation exists. This parameter regime corresponds to a driving impedance higher than a critical value given by Eq. (21). For low voltage (200 – 400 kV) broad area ($S > 100$ cm^2) diodes, such as may be used to pump a gas laser, this critical impedance may be very low as indicated in Fig. 3.

A long pulse, cold cathode e-beam diode requires a sufficiently "stiff" power supply to provide a nearly constant voltage for a sufficiently long period of time for the plasma layer to approach steady state. These stringent requirements are typically not satisfied in cold cathode e-beam systems reported in the literature in which the diode is often driven

by a matched pulse forming line. It should be noted that for the parameters typical of excimer laser diodes, very low plasma electron temperatures ($T_e < 1$ eV) are required in order to bring the critical impedance above the diode impedance in a system in which the driving impedance is matched to the initial space-charge limited diode impedance. Even if the driving impedance condition is satisfied, the driving circuit must be capable of supplying voltage to the diode for several microseconds in order for the plasma layer to approach steady state. An appropriate driving circuit might take the form of a high capacitance Marx bank directly connected to the diode. Alternately, a double-pulsed system may be envisioned in which a cathode plasma, produced by pulsing a very high field stress grid close to the cathode surface, is allowed to expand under field-free conditions until its density profile in the gap closely approximates the desired steady state profile. The extraction potential would then be applied to the anode–cathode gap for a length of time corresponding to the desired current pulse length.

An additional requirement of the steady state plasma model is that the plasma layer be uniform in the transverse dimensions. This condition is not satisfied in many experiments reported in the literature in which nonuniform plasma formation occurs because of enhanced electric fields[2] at cathode edges. Plasma uniformity is also a strong function of cathode material and surface preparation.[14] The existence of a nonuniform plasma layer will significantly change the diode dynamics by altering the dependence of the space-charge limited electron current on the gap spacing.

The existence of a steady state in this model is based on the underlying assumption that plasma is produced only in a uniform region close to the cathode surface whose spatial extent is very small compared to the size of the plasma layer. Clearly, the expansion of the source layer away from the cathode and the slow expansion phase of the plasma layer will compete, and the system may never reach the predicted steady state. The plasma evolution may also be affected by other diode conditions, such as depletion of gas or emission sites at the cathode surface, the accumulation of neutrals in the gap due to charge exchange, the formation of anode plasma, and the growth of hydrodynamic instabilities in the plasma layer. Therefore, the assumptions that lead to the predicted steady state will almost certainly be violated over long periods of time. However, a system that has reached the slow expansion phase predicted by the model may satisfy the practical requirements for a steady state diode. In the example shown in Figs. 5 and 6, for instance, the expansion velocity of the plasma boundary after 2 μsec is less than 0.05 cm/μsec.

ACKNOWLEDGMENTS

The authors would like to thank Dr. Milan Tekula and Dr. Jonah Jacob for many useful discussions.

This work was supported by SDIO/Air Force Aeronautical Systems Division, Contract No. F33615-84-C-2487.

[1] M. Friedman and M. Ury, Rev. Sci. Instrum. **43**, 1659 (1972).
[2] R. K. Parker, R. E. Anderson, and C. V. Duncan, J. Appl. Phys. **45**, 2463 (1974).
[3] R. Schneider, C. Stallings, and D. Cummings, J. Vac. Sci. Technol. **12**, 1191 (1975).
[4] J. G. Kelly and L. P. Mix, J. Appl. Phys. **46**, 1084 (1975).
[5] T. H. Martin and R. S. Clark, Rev. Sci. Instrum. **47**, 460 (1976).
[6] D. W. Swain, S. A. Goldstein, L. P. Mix, J. G. Kelly, and G. R. Hadley, J. Appl. Phys. **48**, 1085 (1977).
[7] V. A. Burtsev, M. A. Vasilevskii, O. A. Gusev, A. B. Efimov, I. M. Roife, E. V. Seredenko, and V. I. Engel'ko, Sov. Phys. Tech. Phys. **23**, 845 (1978).
[8] S. V. Lebedev, V. V. Chikunov, and M. A. Shcheglov, Sov. Tech. Phys. Lett. **8**, 302 (1982).
[9] J. J. Ramires and D. L. Cook, J. Appl. Phys. **51**, 4602 (1980).
[10] D. Hinshelwood, PhD. thesis, MIT, 1985; and references therein.
[11] S. P. Bugaev, G. A. Mesyats, and D. I. Proskurovskii, Sov. Phys. Dokl. **14**, 605 (1969).
[12] M. A. Vasilevskii, I. M. Roife, and V. I. Engel'ko, Sov. Phys. Tech. Phys. **26**, 671 (1981).
[13] H. F. Ivey, J. Appl. Phys. **23**, 208 (1952).
[14] R. E. Klinkowstein and R. E. Shefer, Bull. Am. Phys. Soc. **31**, 1396 (1986).